



UNIVERSITY OF LEEDS

This is a repository copy of *A colorimetric hydrogen sulfide sensor based on gellan gum-silver nanoparticles bionanocomposite for monitoring of meat spoilage in intelligent packaging*.

White Rose Research Online URL for this paper:
<http://eprints.whiterose.ac.uk/149443/>

Version: Accepted Version

Article:

Zhai, X, Li, Z, Shi, J et al. (10 more authors) (2019) A colorimetric hydrogen sulfide sensor based on gellan gum-silver nanoparticles bionanocomposite for monitoring of meat spoilage in intelligent packaging. *Food Chemistry*, 290. pp. 135-143. ISSN 0308-8146

<https://doi.org/10.1016/j.foodchem.2019.03.138>

© 2019 Elsevier Ltd. All rights reserved. Licensed under the Creative Commons Attribution-Non Commercial No Derivatives 4.0 International License (<https://creativecommons.org/licenses/by-nc-nd/4.0/>).

Reuse

This article is distributed under the terms of the Creative Commons Attribution-NonCommercial-NoDerivs (CC BY-NC-ND) licence. This licence only allows you to download this work and share it with others as long as you credit the authors, but you can't change the article in any way or use it commercially. More information and the full terms of the licence here: <https://creativecommons.org/licenses/>

Takedown

If you consider content in White Rose Research Online to be in breach of UK law, please notify us by emailing eprints@whiterose.ac.uk including the URL of the record and the reason for the withdrawal request.



eprints@whiterose.ac.uk
<https://eprints.whiterose.ac.uk/>

1 Natural biomaterial-based edible and pH-sensitive films combined with
2 electrochemical writing for intelligent food packaging

3 Xiaodong Zhai^{†,1}, Zhihua Li^{†,1}, Junjun Zhang^{†,1}, Jiyong Shi^{†,1}, Xiaobo Zou^{*,†,1}, Xiaowei
4 Huang^{†,1}, Yue Sun^{†,1}, Wen Zhang^{†,1}, Zhikun Yang^{†,1}, Mel Holmes^{‡,1}, Yunyun Gong^{‡,1},
5 Povey, Megan J^{‡,1}

6 [†]Agricultural Product Processing and Storage Lab, School of Food and Biological
7 Engineering, Jiangsu University, Zhenjiang, Jiangsu 212013, China

8 [‡]School of Food Science and Nutrition, the University of Leeds, Leeds LS2 9JT,
9 United Kingdom

10 ¹China-UK joint laboratory for nondestructive detection of agro-products, Jiangsu
11 University, Zhenjiang, Jiangsu 212013, China

12 * Corresponding author. Tel.: +86 511 88780174; fax: +86 511 88780201; Email:
13 zou_xiaobo@ujs.edu.cn

14 **ABSTRACT**

15 An edible and pH-sensitive film combined with electrochemical writing was developed
16 using gelatin, gellan gum and red radish anthocyanin extract for intelligent food packaging
17 applications. The composite film displays orange red-to-yellow color change over the pH
18 range 2-12. The tensile strength, ductility, and barrier response of the films to UV light and
19 oxygen improved with the increase of red radish anthocyanin concentration. Multicolor
20 patterns were successfully drawn on the film using an electrochemical inscribing method.
21 The composite films acted as gas sensors which presented visible color changes in the
22 presence of milk and fish spoilage, while the written patterns were well preserved.
23 Accordingly, this composite film with written patterns could be an easy-to-use indicator
24 with great potential for monitoring food spoilage as part of an intelligent packaging system.

25 **KEYWORDS: intelligent food packaging; gelatin; gellan gum; red radish**
26 **anthocyanins; electrochemical writing; film**

27 **1. INTRODUCTION**

28 Intelligent food packaging has received great interest in the last decades, because of
29 their potential for monitoring the condition of packaged foods or the surrounding
30 environment.¹ Generally, intelligent food packaging systems can be realized by three main
31 technologies, namely sensors, indicators and data carriers.² Among these systems,
32 indicators (e.g. freshness indicators, time-temperature indicators and gas indicators) which
33 could provide qualitative or semi-quantitative information by means of a color change have
34 been widely studied since they are easy to fabricate and can be read by the naked eye.

35 In recent years, many pH-sensitive indicators have been developed to monitor food
36 quality. This was because various non-neutral volatile gases, such as amines, hydrogen
37 sulfide and carbon dioxide, can be generated from foods during spoilage. When these
38 volatile gases diffused to the headspace of the packages, they could react with the pH-
39 sensitive indicators causing color changes of the indicators. Generally, the pH-sensitive
40 materials were composed of pH dyes and a solid matrix to immobilize the pH dyes.^{3, 4}
41 Concerning that traditional synthetic pH dyes with potential harmful effects to human
42 beings are not ideal for food packaging,⁵ more attention has recently been paid to natural
43 and safe coloring agents, such as anthocyanins⁶⁻¹⁴ and curcumin.¹⁵⁻¹⁸ In addition, the public
44 concern over environmental pollution caused by plastics has driven a greater demand for
45 packaging materials to be eco-friendly by using biopolymers with good film-forming
46 properties, such as starch, chitosan, gums, alginate, agar, gelatin and so forth.

47 Red radish (*Raphanus sativus* L.) (RR) is a anthocyanins-rich vegetable,¹⁹ in which
48 anthocyanins mainly exist at acylated structures.²⁰ Anthocyanins extracted from red radish

49 are widely used as natural safe food-coloring agents because of their high stability and their
50 orange-red color similar to that of synthetic Food Red No. 40.^{20,21} As red radish is readily
51 available at low cost, the red radish anthocyanins (RRA) is a good resource of pH-sensitive
52 dye. The solid matrix used to immobilize anthocyanins is also a critical component of a
53 sensitive, safe and yet environment sustainable indicator. Gelatin is a denatured protein
54 from the triple helix of collagen. It is accepted as “Generally Recognized as Safe” (GRAS)
55 food additives by the US Food and Drug Administration (FDA).²² Gelatin is considered as
56 a promising natural polymer for packaging applications because of its renewability,
57 biodegradability and film-forming property.²³ in particularly with good oxygen barrier
58 property.²² This may be used to protect packaged foods from being oxidized and thus
59 improve their shelf life. However, poor mechanical properties (such as frangibility) have
60 been described as one of the disadvantages of gelatin films.²⁴ To compensate this
61 shortcoming, gelatin is generally cross-linked and/or combined with other polymers, such
62 as sodium alginate ²⁵ and chitosan.²⁶ Gellan gum is a linear negatively charged
63 biodegradable exopolysaccharide. Four repeating carbohydrates are present in the main
64 chain of gellan gum, which includes two d-glucose carbohydrates, one L-rhamnose, and
65 one D-glucuronic acid.²⁷ It is safe to use with acceptable daily intake (ADI) dose not
66 specified, and has received both US FDA and EU (E418) approval for application mainly
67 as a multi-functional gelling, stabilizing and suspending agent in a variety of foods and
68 personal care products.²⁸ Importantly, it was found that not only the mechanical properties
69 of gelatin film could be significantly improved by gellan gum,²⁹ also the gellan gum could
70 enhance the thermal stability of anthocyanins according to a new study.³⁰ Hence, the

71 gelatin/gellan gum blend is considered a preferred film-forming agent to immobilize
72 anthocyanins.

73 Most food packaging materials are labelled in order to provide information about the
74 packaged foods and inks are typically derived from petrochemical feedstock, which brings
75 significant environmental sustainability concern to modern society.³¹ In addition, the
76 migration of unsafe printing inks from packaging to food can be a risk for consumers
77 health.³² To solve these problems, new inks such as edible inks and new techniques for
78 printing are very desirable.³³ Recently, Wu, et al.³⁴ successfully printed on polysaccharide
79 film by an electrochemical method based on the pH response color change of anthocyanins.
80 As anthocyanins are safe and biodegradable, this electrochemical writing can be regarded
81 as a green printing method. However, the related work of electrochemical writing on edible
82 films is still limited.

83 In this study, we aimed to develop a new pH-sensitive and edible film by using RRA as
84 the pH-sensitive pigment and gelatin/gellan gum blend as the film-forming agent,
85 respectively. The fundamental properties of films, such as microstructure, mechanical
86 properties and gas permeability properties were first investigated. Then, multicolor patterns
87 were inscribed on this polysaccharide/protein composite film by using an electrochemical
88 deposition method. Finally, the film combined with deposited patterns was used to indicate
89 milk and fish quality.

90 **2. MATERIALS AND METHODS**

91 **2.1. Materials and Reagents.** Fresh red radish (cultivar ‘Xinlimei’) and live black carp
92 were purchased from local market, and pasteurized milk was purchased from a local cattle

93 farm (Zhenjiang, China). Gelatin (type B, pig skin) was purchased from Sigma-Aldrich Inc.
94 (St. Louis, MO, USA). Low-acyl gellan gum was purchased from Dancheng Caixin sugar
95 industry Co., Ltd. (Dancheng, China). Other chemical agents, such as ethyl alcohol, calcium
96 chloride, acetic acid, ammonium hydroxide, acetonitrile and formic acid were bought from
97 Sinopharm Chemical Reagent Co., Ltd (Shanghai, China).

98 **2.2. Extraction of anthocyanins from red radish.** Fresh red radishes were peeled, cut
99 into pieces and dried at 65 °C under vacuum. Then, the dried red radishes were crushed
100 into powder and transferred to 80% ethanol aqueous solution with a solid-liquid ratio of
101 1:10. After stirring at 35 °C for 6 h, supernatant of the solution was collected through
102 filtration using a 25- μ m filter paper. Ethanol in the supernatant was removed with a vacuum
103 rotary evaporator at 45 °C in dark conditions. Finally, the concentrated RRA extract
104 solution was freeze-dried under vacuum and the RRA extract powder obtained was stored
105 at 4 °C in a brown bottle filled with nitrogen.

106 The anthocyanin content in lyophilized RRA extract powder was measured by the pH
107 differential method.³⁵ Absorbance of sample at 520 and 700 nm was measured using a UV-
108 Vis spectrophotometry (Agilent CARY 100, Varian Corporation, USA). The anthocyanin
109 content was expressed in mg/g.

110 **2.3. Preparation of films.** Firstly, 100 mL aqueous dispersion containing 3 g of gelatin
111 (G) and 1 g of gellan gum (GG) was heated at 85 °C in a water bath and stirred with a
112 magnetic stirrer for 0.5 h to form a clear solution. Under this constant temperature, 30 mg
113 of CaCl₂·2H₂O was added into the solution with continuous stirring. Based on the
114 calculated anthocyanins content (303.42 ± 7.82 mg/g) (refer to section 2.3), RRA extract

115 powder was then added to the solution to obtain an anthocyanin contents of 5 mg/100 mL,
116 10 mg/100 mL, 15 mg/100 mL and 20 mg/100 mL, expressed as RRA5, RRA10, RRA15
117 and RRA20. A control solution containing gelatin, gellan gum and $\text{CaCl}_2 \cdot 2\text{H}_2\text{O}$ was also
118 prepared. After degassing with a sonicator at 85 °C, 12 g of the film-forming solution was
119 immediately poured into a clean and smooth plastic Petri dish with a 9 cm diameter. Then,
120 firm hydrogels were formed after the solutions were cooled down. The hydrogels were
121 dried to films by putting the Petri dishes on a horizontal platform in an oven at 45 °C for 2
122 h. After that, the film was peeled from the Petri dishes and stored in an incubator at 4 °C
123 with 75% RH for further use.

124 In order to prepare films with electrochemical writing, the above-mentioned hydrogels
125 containing RRA were firstly taken out from the Petri dish before drying. The hydrogel was
126 placed in contact with a platinum (Pt) plate connected to the cathode of an electrochemical
127 analyzer (CHI660E, CH Instruments Co., Shanghai, China). Then, a Pt needle (diameter
128 0.5 mm) connected to the anode of the electrochemical analyzer touched the upper surface
129 of the hydrogel. Under a constant current, hydrogen ions were produced around the
130 platinum needle and thus induced an orange red color of RRA. On the contrary, when the
131 Pt plate was connected to the anode of the electrochemical analyzer and the Pt needle was
132 connected to the cathode of the electrochemical analyzer, hydroxyl ions were produced
133 around the Pt needle and thus induced a green color of RRA. The movement of the platinum
134 needle was procedurally controlled by a mechanical arm with a step precision of 0.1 μm
135 (DOBOT M1, Shenzhen Yuejiang Technology Co., Ltd, China). The hydrogel was
136 immediately dried in a vacuum-drying oven at 70 °C to form a film which was stored at
137 4 °C with 75% RH prior to use.

138 **2.4. Characterization of the films**

139 **2.4.1. Color response to pH variation.** UV-vis spectra of films were measured using a
140 UV-vis spectrophotometer (Agilent CARY 100, Varian Corporation, USA). Firstly, pH
141 buffer solutions (pH 2-12) were prepared by using 0.2 M disodium hydrogen phosphate,
142 0.2 M citric acid and 0.2 M sodium hydroxide solutions with different proportions. Then,
143 films were cut into squares (1 cm × 1 cm) and immersed in the buffer solutions for 5 min.
144 The spectra of the films in the range of 400-800 nm wavelength were obtained using air as
145 the reference blank.

146 **2.4.2. Microstructure observation.** The micrographs of the films were recorded by a
147 field emission scanning electron microscope (FE-SEM) (S-4800, Hitachi High
148 Technologies Corporation, Japan). The films were first freeze fractured by liquid nitrogen
149 before measurement. Samples were attached to double-sided adhesive tape and mounted
150 on the specimen holder, then sputtered and coated with gold under vacuum.

151 **2.4.3. Mechanical properties.** Tensile strength (TS) and elongation-at-break (EB) of the
152 films were measured with an Instron Universal Testing Machine (Model 4500, Instron
153 Corporation, Canton, MA, USA) using a modified ASTM D882-00 (ASTM, 2000b)
154 procedure. Samples were conditioned at 25 °C and 50 ± 3% RH in a desiccator containing
155 magnesium nitrate saturated solution for 2 d prior to analysis. Each film was cut in
156 rectangular strips with 60 mm length and 20 mm width. The initial grip separation and
157 crosshead speed were set at 40 mm and 0.6 mm s⁻¹ respectively. The TS and EB were
158 calculated as the equation (1) and (2), respectively. Measurements represent an average of
159 six samples.

160 $TS = F_{\max} / S$ (1)

161 $E (\%) = 100 \times \Delta l / l_0$ (2)

162 where TS was the tensile strength (MPa); F_{\max} was the maximum load (N); S was the
163 initial cross-sectional area of the film sample (mm^2); E was the elongation-at-break; Δl was
164 the extension of the film (mm) and l_0 was the initial test length of the film (40 mm).

165 **2.4.4. Transparency measurement.** The optical transmittance of GGG and GGG-RRA
166 films ($2 \text{ cm} \times 1 \text{ cm}$) were measured in the range of 200–800 nm with air as the reference
167 blank by using the UV–vis spectrophotometer.

168 **2.4.5. Water vapor permeability.** Water vapor permeability (WVP) of films was
169 determined gravimetrically using a standard test method (ASTM E96-05). The film
170 samples that had previously equilibrated at 50% RH for 48 h were sealed on glass cups
171 containing dried silica gel (0% RH). The cups were then placed in desiccators containing
172 saturated $\text{Mg}(\text{NO}_3)_2$ solution (50% RH) at 25 °C. The cups were weighed at 1-h interval
173 until a steady state was reached. The water vapor transmission rate (WVTR) of a film was
174 determined from the slope of the regression analysis of weight gain of moisture (Δm) that
175 transferred through a film area (A) during a definite time (t), as shown in equation (3). Then,
176 the WVP of the film was calculated based on the WVTR, as shown in equation (4).
177 Measurements represent an average of six samples.

178 $WVTR = \Delta m / (A \times t)$ (3)

179 $WVP = WVTR \times x / \Delta P$ (4)

180 where Δm is the weight gain of the cup (g); x is the film thickness (m); A is the exposed
181 area (m^2); ΔP is the partial water vapor pressure difference across the film (1583.7 Pa at
182 25°C); t is the time (h).

183 **2.4.6. Oxygen permeability.** Oxygen permeability (OP) of the film was estimated at
184 25°C and 50% RH with an automated oxygen permeability testing machine (GTR-7001,
185 SYSTESTER, China) following the standard method (ASTM D3985-05, 2005). Film was
186 placed on a stainless-steel mask with an open testing area of 48 cm^2 . Oxygen and nitrogen
187 were respectively flowed on each side of the films. Oxygen transmission rate (OTR) was
188 measured and OP was calculated according to equation (5). Measurements represent an
189 average of six samples.

$$190 \quad \text{OP} = \text{OTR} \times x / \Delta P \quad (5)$$

191 where OTR is the oxygen transmission rate ($\text{cm}^3 \cdot \text{m}^{-2} \cdot \text{d}^{-1}$); x is the film thickness (m); ΔP is
192 the partial pressure of oxygen (1.013×10^5 Pa at 25°C).

193 **2.4.7. Color stability.** The colorimetric films were stored in incubators at 4°C and 25°C
194 with 75% RH under fluorescent lights. The images of the colorimetric films were captured
195 every day for two weeks by an optical scanner (Scanjet G4050, HP) and analyzed by a user
196 program in Matlab R2012a (Matworks Inc., Natick, MA, USA). The stability of the
197 colorimetric films was defined as the relative colour change, according to our previous
198 study:³⁶

$$199 \quad \Delta R = |R_0 - R_1| \quad (6)$$

200 $\Delta G = |G_0 - G_1|$ (7)

201 $\Delta B = |B_0 - B_1|$ (8)

202 $S = (\Delta R + \Delta G + \Delta B) / (R_0 + G_0 + B_0) \times 100\%$ (9)

203 where R_0 , G_0 , B_0 were the initial gray values of the red, green and blue, R_1 , G_1 , B_1 were the
204 gray values of the red, green and blue after storage. S was the relative color change of R ,
205 G and B values.

206 **2.4.8. Color response to basic and acid gases.** Response of the colorimetric films
207 toward volatile ammonia in term of their color changes was performed using absorbance
208 measurements. The colorimetric films were hang up in an Erlenmeyer flask (500 mL) at 1
209 cm above the ammonia solution (80 mL, 8 mM) at 25°C.

210 **2.5. Application of films in monitoring food quality**

211 **2.5.1. Milk spoilage trial.** 20 mL of pasteurized fresh milk was poured into an unused
212 plastic Petri dish (diameter 90 mm) with a lid. In the middle of the lid, a square hole was
213 cut using a knife. Then the film was fixed on the lid to cover the hole. The Petri dish was
214 sealed with Vaseline and placed in an incubator at 25 °C with 75% RH. During milk
215 spoilage, volatile gases were generated from the milk and diffuse through the film, making
216 a color change of the film. The images of the film were captured using the optical scanner.
217 The acidity of milk was measured by acid-base titration method according to a previous
218 literature.³⁷

219 **2.5.2. Fish spoilage trial.** Fresh black carp (*Mylopharyngodon piceus*) was cut into
220 strips after removing its innards, head, tail and scales. Like the milk spoilage trail, 25 g of
221 black carp was put into the plastic Petri dish and the film was fixed on the lid to cover the
222 hole. The Petri dish was placed in an incubator at 4 °C with 75% RH. The total volatile
223 basic nitrogen (TVB-N) content was measured according to a previous literature.³⁸

224 **3. RESULTS AND DISCUSSION**

225 **3.1. Color and UV-vis spectra of RRA and GGG-RRA film.** In this study, RRA was
226 used as the pH-sensitive pigment to develop packaging films, so the color response of RRA
227 and GGG-RRA film to pH variation was firstly investigated. Fig. 1A shows that RRA
228 solutions changed from orange red to yellow when pH increased from 2 to 12. In detail,
229 RRA solution turned from deep orange red to light orange over the pH range of 2-7. At
230 weak basic conditions, the color became purple (pH 8-9). Then, the color changed to yellow
231 green (pH 10) and finally to yellow (pH 10-12). Corresponding to color changes in RRA
232 solutions, the maximum absorption peak presented red-shifts. As shown in Fig. 1B, the
233 maximum absorption peak obtained at pH 2 was around 510 nm, which gradually shifted
234 to 520 nm when the pH increased to 6. Meanwhile, the maximum absorption values
235 decreased. As the pH increased over 7, the maximum absorption peak shifted to
236 approximately 580 nm. At the same time, the absorption values gradually increased when
237 pH increased from 7 to 10 and then decreased when pH increased from 10 to 12. The
238 absorbance ratio at 580 nm versus 510 nm (A_{580}/A_{510}) indicates the increase of green
239 intensity compared to red. The calibration curve (Fig. 1B inset) showed that values of
240 A_{580}/A_{510} in PSPE solution increased and then decreased over the range of pH 2-9. An
241 exponential calibration curve was established between the pH in the range of 2-9 and

242 A_{580}/A_{510} of the RRA solution, as formula (10), where x and y were the pH and A_{580}/A_{510} ,
243 respectively.

$$244 \quad y = 0.1399e^{0.2745x}, R^2 = 0.9823 \quad (10)$$

245 The GGG film containing RRA showed similar color (Fig. 1C) and spectra (Fig. 1D)
246 changes with RRA in response to pH variation. An exponential calibration curve was also
247 established between the pH in the range of 2-9 and A_{580}/A_{510} of the GGG-RRA film (Fig.
248 1D inset), according to the formula (11), where x and y were the pH and A_{580}/A_{510} ,
249 respectively.

$$250 \quad y = 0.2911e^{0.1583x}, R^2 = 0.9791 \quad (11)$$

251 Similar exponential calibration curves were also found in anthocyanins extracted from
252 purple sweet potato (PSP) and film containing PSP anthocyanins.³⁹ The exponential
253 calibration curve between pH and A_{580}/A_{510} for the GGG-RRA film indicated that RRA
254 maintained good chemical activity in the GGG film. The visible color changes of GGG-
255 RRA film toward pH change implied it was capable of indicating pH-related food quality.

256 **3.2. Microstructure of the films.** The SEM images showed that GGG film had a highly
257 compact and dense appearance of cross section (Fig. 2A). This indicated that gelatin and
258 gellan gum had excellent compatibility with each other due to the intermolecular
259 interaction. Similar homogeneous structure of composite G and GG film was also observed
260 in a previous study.⁴⁰ When a low content of RRA (i.e. 5 mg/100 mL) was added into the
261 GGG film, some small spindrift-like structures appeared and was uniformly distributed in
262 the film (Fig. 2B). With the increase of RRA content, the GGG-RRA films showed obvious

263 aggregation of spindrift-like structures and stratification (Fig. 2C and Fig. 2D). When a
264 relatively high content of RRA was added, the GGG-RRA20 film in turn became more
265 uniform than the GGG-RRA10 and GGG-RRA15 film even though the size of spindrift-
266 like structures was larger (Fig. 2E). This phenomenon could be explained by the gelation
267 process of both gelatin and gellan gum. During the gelation formation of gelatin, junction
268 zones were formed by small segments of two or three polypeptide chains reverting to the
269 collagen triple helix-like structure.⁴¹ It has been reported that the addition of phenolic
270 compounds promote the formation of hydrogen bonds among the three helices.⁴² For the
271 gellan gum, the formation of gels was closely affected by the pH of the solution. As gellan
272 gum is a linear anionic polysaccharide, the aggregation of gellan gum helices in water was
273 impeded by the intermolecular repulsion between negatively charged carboxylic groups on
274 the gellan gum, while this intermolecular repulsion can be weakened with the decrease of
275 pH of the solution, resulting in an enhancement of junction zone formation.⁴³ In this study,
276 RRA as a phenol compound could also contribute to the gelation of gelatin. At the same
277 time, with the increase of the RRA content, the pH of the solution decreased, contributing
278 the gelation of gellan gum. Therefore, more intermolecular cross-linking within gelatin
279 molecules and gellan gum molecules were generated, leading to partial phase separation of
280 gelatin and gellan gum. As shown in Fig. 2B-D, the continuous and compact phase with
281 parallel-arranged long chains could largely comprise gelatin molecules, while the coarse
282 phase could largely comprise gellan gum. However, when the RRA content was at a
283 relatively high level (20 mg/100 mL), the phase separation between gelatin and gellan gum
284 molecules in the GGG-RRA20 film was not as obvious as that in the GGG-RRA10 and

285 GGG-RRA15 films. This might be due to excessive RRA having a steric hindrance effect
286 on the formation of crosslinks among gelatin and gellan gum chains.

287 **3.3. Mechanical and barrier properties.** TS represents the capacity of the films to
288 withstand loads tending to elongate and EB expresses the capability of the films to resist
289 changes of shape without crack formation. The TS and EB of the GGG and GGG-RRA
290 films are shown in Fig. 3A. With the increase of RRA content, the TS and EB of the films
291 both become higher, indicating improved coupling strength and ductility of the films. The
292 changes in mechanical properties of the films could be explained by the intermolecular
293 interaction of G and GG in the absence and presence of RRA. The higher TS of the films
294 in the presence of RRA could be due to the enhanced cross-linking among G and GG chains,
295 respectively, as mentioned in section 2.3. Generally, an improved TS of a film was
296 accompanied by a sacrifice of EB. However, the EB of the GGG-RRA films also increased
297 with the increase of RRA. This could be due to the layer structure of the GGG-RRA films
298 that endowed them with better flexibility compared to the GGG film.

299 Fig. 3B shows the UV-vis transmission spectra and images (inset) of GGG and GGG-RRA
300 films. Pure GGG film was colorless and had a transparency of over 80% in the visible range
301 of 400-800 nm. The incorporation of RRA into GGG film resulted in an orange color which
302 became deeper with the increase of RRA content. The barrier property of the film to UV
303 light could be obtained from the spectra in the range of 200-400 nm. GGG film presented
304 excellent barrier properties to UV light in the range of 200-245 nm where the
305 corresponding transparencies were lower than 1%, similar to a previous gelatin film.⁴⁴
306 Moreover, the UV light barrier ability of the films were significantly enhanced with RRA,
307 since the films with higher RRA content showed improved barrier ability over broader

308 spectra ranges. GGG-RRA20 film presented strong barrier ability to UV light in the range
309 of 200-360 nm. These results could be due to the fact that RRA as a phenolic compound is
310 favorable for the adsorption of UV radiation.⁴⁵ The good UV light barrier properties of
311 GGG-RRA films may be beneficial for food preservation because UV light is known to
312 induce deleterious change, particularly lipid oxidation, in foods.⁴⁶

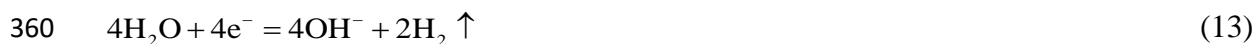
313 Fig. 3C shows the effect of RRA on the WVP of GGG films. Pure GGG film had a WVP
314 value of 2.83 g mm m⁻² kPa⁻¹ h⁻¹, which was several orders of magnitude higher than that
315 of polyethylene (PE) and poly(vinylidene chloride) (PVDC) films.⁴⁷ The high WVP of
316 GGG film could be due to the hydrophilic nature of gelatin and gellan gum. With the
317 increase of RRA content, the WVP of the films presented a first decline followed by a rise.
318 For GGG-RRA10 film, the WVP was 1.25 g mm m⁻² kPa⁻¹ h⁻¹, which was lower than a
319 half of the WVP value of the GGG film. As the RRA content increased to 20 mg/ 100 mL,
320 the GGG-RRA20 film showed a comparable WVP (3.17 g mm m⁻² kPa⁻¹ h⁻¹) to the GGG
321 film. The permeability of a film largely depends on its chemical structure, morphology and
322 hydrophilicity, regardless of the environment conditions. The initial decrease of WVP of
323 films with the increase of RRA content to 10 mg/ 100 mL could be due to anthocyanin
324 enhancement of the interactions of both gelatin and gellan gum molecules, lowering the
325 amount of gelatin and gellan gum molecules needed to form hydrophilic bonding with
326 water and subsequently leading to a decrease in the affinity of the films towards water.
327 Meanwhile, anthocyanins as phenolic components could form mainly non-covalent
328 hydrophobic interactions with gelatin and gellan gum⁴⁸ and thus reduce the hydrophilicity
329 of the films. However, a significant increase of WVP of the film was observed from the
330 GGG-RRA15 and GGG-RRA20 films. This may be due to the high hydrophilicity of

331 anthocyanins that made the film easier to absorb water when RRA content was too high.
332 Hence, the results indicated that addition of a relatively low content of RRA in the GGG
333 film beneficially lowered its mainly consequently reducing the water evaporation of
334 packaged foods.

335 The GGG film had an oxygen permeability (OP) of $10.05 \text{ cm}^3 \mu\text{m m}^{-2} \text{ d}^{-1} \text{ kPa}^{-1}$ (Fig. 3D),
336 which was much lower than low density polyethylene (LDPE) ($1900 \text{ cm}^3 \mu\text{m m}^{-2} \text{ d}^{-1} \text{ kPa}^{-1}$)
337 and higher than poly(vinylidene chloride) (PVDC) ($0.1\text{--}3 \text{ cm}^3 \mu\text{m m}^{-2} \text{ d}^{-1} \text{ kPa}^{-1}$) and
338 ethylene-vinyl alcohol copolymers (EVOH) ($0.77 \text{ cm}^3 \mu\text{m m}^{-2} \text{ d}^{-1} \text{ kPa}^{-1}$), but comparable
339 to polyvinyl chloride (PVC) ($20\text{--}80 \text{ cm}^3 \mu\text{m m}^{-2} \text{ d}^{-1} \text{ kPa}^{-1}$)⁴⁹. The increase of RRA content,
340 caused the OP value of GGG-RRA films to slightly decrease to $6.33 \times 10^{-2} \text{ cm}^3 \mu\text{m m}^{-2} \text{ d}^{-1}$
341 kPa^{-1} (GGG-RRA20 film). The OP of the films was closely related to the diffusion path
342 of oxygen within the film. The decrease of OP resulting from the increase in RRA content
343 could be due to that the stronger crosslinking of gelatin and gellan gum leading to a
344 reduction of the free volume for oxygen to pass through the films. The low OP of the GGG-
345 RRA films may reduce the oxidation content of packaged foods.

346 **3.4. Electrochemical writing on GGG-RRA film.** In order to write information on the
347 films using the electrochemical method, a hydrogel needed to be firstly fabricated. In this
348 study, a firm gel with a good toughness was facilely formed after the GGG-RRA solution
349 was cooled down without further treatment (Fig. 4A), attributed to the good gelation ability
350 of gelatin and gellan gum. It is well known that the color of anthocyanins is dependent on
351 pH condition⁵⁰, so the principle of electrochemical writing on the hydrogel can be
352 expressed as in scheme 1. When the Pt needle was connected to the anode of the
353 electrochemical workstation, a localized low pH condition was generated in the hydrogel

354 due to the anodic water electrolysis reaction (equation 12) so that anthocyanins turned to
355 acid color (orange red). On the contrary, when the Pt needle was connected to the cathode
356 of the electrochemical workstation, a localized high pH condition was generated in the
357 hydrogel due to the cathodic water electrolysis reaction (equation 13) and therefore
358 anthocyanins turned to basic color (yellow).



361 The movement of the Pt needle along the horizontal plane was controlled by a mechanical
362 arm to produce desired patterns. After being written on the hydrogels, the patterns were
363 preserved by immediately drying the hydrogels to films. Apart from the current direction,
364 the current magnitude could also make the color of the patterns different. When the current
365 increased from 1 to 6 mA, the pattern “1” turned more acid (Fig. 4B) or basic colors (Fig.
366 4C). This was because a greater current led to more intense water electrolysis reaction and
367 thus a greater acid or basic condition. Accordingly, multicolor patterns could be written on
368 one film by tuning the current direction and magnitude. As shown in Fig. 4D and 4E, the
369 flower with orange red petals and green calyces, and the apple with orange red fruit and
370 yellow leaves were respectively drawn on individual films.

371 **3.5. Color stability and gas sensing ability.** The stability of the films and the written
372 patterns are of great importance for the practical application of the films. Fig. 5A shows
373 the images of the GGG-RRA10 film with red and yellow patterns stored at 75% for 30 d
374 at 4, 25 and 37 °C. The color of the film and patterns gradually faded during storage.
375 Especially at a higher temperature (37 °C), the film obviously turned less red and the

376 patterns discolored significantly after 30 d. To describe the degree of discoloration, the
377 relative color change (S) of the film and patterns was tested and shown in Fig. 5B. The S
378 values of films and patterns increased slightly overall. In contrast, the S values were higher
379 at a higher temperature for both the film and the patterns. At a certain temperature, the S
380 values of the yellow pattern were higher than that of the red pattern followed by the film,
381 indicating that the film had greater color stability than the red pattern and then the yellow
382 pattern. Generally, the anthocyanins are more stable at lower pH.⁵¹ The reason why the red
383 pattern was less stable than the film remained unclear.

384 Before the film was employed as a gas sensor in the packaging system, its sensing ability
385 to acid and basic gas were investigated. As shown in Fig. 5C and 5D, the GGG-RRA film
386 gradually turned to redder after exposure to acetic acid gas, and turned to green after
387 exposed to ammonia gas. This result suggested that the GGG-RRA film could be used to
388 indicate the food spoilage when either acid or basic gases were the dominant volatile gases.
389 As for the written patterns on the film, the red triangle maintained its original color in
390 response to acetic acid (Fig. 5C) but gradually faded in response to ammonia (Fig. 6D). At
391 the same time, the yellow triangle maintained yellow in response to ammonia (Fig. 6D)
392 while gradually fading in response to acetic acid (Fig. 6C). Hence, to keep the written
393 information stable on the film, the films with both? red color patterns and yellow patterns
394 could be used to indicate food spoilage during which acid gases and basic were the main
395 volatile gases, respectively.

396 **3.6. Application of films for indicating milk and fish spoilage.** In this study, the GGG-
397 RRA10 film was selected to indicate food quality, considering the effect of the
398 anthocyanins concentration on the color visibility and gas sensitivity of the films discussed

399 in our previous study.¹² The GGG-RRA10 films with red pattern “F” and yellow pattern
400 “F” were used to monitor milk and fish spoilage, respectively. As shown in Fig. S1, the
401 films were fixed on the lid to cover the hole that worked as the detection window through
402 which the volatile gases generated from milk and fish diffused to contact with the film and
403 make a color change of the film. In this way, the water vapor inside of the dishes could
404 permeate through the film to the external environment to reduce the film swelling that
405 might cause anthocyanins to leach from the film.

406 Fig. 6A shows the color change of the GGG-RRA10 film during the milk spoilage. With
407 the increase of time, the film turned to be redder. The color change could also be seen from
408 the color parameters, namely red (R), green (G) and blue (B). As shown in Fig. 6B, the R
409 value increased from 232 to 253, indicating a deeper red color, while G and B value did
410 not significantly change. The color change of the film implied that acid volatile gases were
411 generated during the milk spoilage. Similar phenomena were also observed in a previous
412 study.¹³ This was largely due to the generation of organic acids during anaerobic respiration
413 of anaerobic bacteria or facultative anaerobic bacteria under hypoxic or anaerobic
414 condition. It is worth mentioning that the low OP of GGG-RRA10 film might contribute
415 to a hypoxic condition for the anaerobic respiration of spoilage bacteria. The acidity of the
416 milk was an important index to evaluate the freshness of milk. A higher acidity value
417 indicated a larger amount of acid components and therefore an inferior freshness. As shown
418 in Fig. 6B, the acidity of the milk increased from 14.78 to 25.67 °T after a 48 h storage at
419 25 °C. According to Chinese standard (GB 19645-2010), the acidity value of pasteurized
420 milk should be under 18 °T to ensure quality. In this study, the acidity of the milk reached

421 at 18 °T for 25 h, while at this point the R value of the film was nearly 240. This implied
422 that if the R value of the film was higher than 240, the milk sample should not be consumed.

423 Fig. 6C shows the color change of the GGG-RRA10 film during the spoilage of black
424 carp. The film gradually turned from initial orange red to green (4 d) and then yellow green
425 (8 d). Accordingly, the color parameter R decreased, and G increased from 0 d to the 4 d
426 (Fig. 6D). However, the R and G value did not dramatically change after 4 d. Meanwhile,
427 the B value decreased over time from initial an 144 to final 18, indicating a deeper yellow
428 color (the complementary color of blue). Hence, the B value could be used as a
429 characteristic parameter for the color change of the film. The color change of the film could
430 be mainly induced by the volatile basic gases, such as ammonia, trimethylamine and
431 dimethylamine, generated from the black carp. Fig. 6D shows the TVB-N content of the
432 black carp. It rose from 4.74 mg/100g at 0 d to 53.71 mg/100g at 9 d at 4 °C. The generation
433 of TVB-N was due to the decomposition of proteins by bacteria and enzymes. According
434 to Chinese Standard (GB 2733-2015), the rejection limit of TVB-N level for black carp is
435 20 mg/100 g. In this study, the TVB-N value rose to 20 mg/100 g at nearly 5.5 d, when the
436 B value of the film was around 87. This implied that if the B value of the film was lower
437 than 87, then the fish sample should not be consumed.

438 For the written patterns “F” on the GGG-RRA10 films that were used for either milk or
439 fish spoilage, as expect, they retained a clear color and shape (Fig. 6A and 6C). As can be
440 seen from the Fig. S2A, R, G, and B values of the red “F” did not obviously change,
441 indicating a good color stability. Although the B value of the yellow “F” significantly
442 decreased (Fig. S2B), the pattern “F” still kept a bright yellow color because of the weak

443 fluctuation of R and G values. Hence, the GGG-RRA film combined with written pattern
444 could be used to indicate the milk and fish spoilage.

445 As mentioned above, when the GGG-RRA-10 film was used to indicate the milk and
446 fish spoilage, the film showed visible color changes while the written patterns on the film
447 maintained good shapes and colors. As the GGG-RRA films were made from degradable
448 and edible biomaterials, and the patterns were in situ drawn on the films by using
449 electrochemical method without the need of inks, they should have a great potential for
450 practical application in intelligent food packaging.

451 **ACKNOWLEDGMENT**

452 The authors gratefully acknowledge the financial support provided by the Postgraduate
453 Research & Practice Innovation Program of Jiangsu Province (KYCX17_1798), the
454 National Science and Technology Support Program (2015BAD17B04), the National Key
455 Research and Development Program of China (2016YFD0401104), the National Natural
456 Science Foundation of China (31671844, 31601543), China Postdoctoral Science
457 Foundation (2013M540422, 2014T70483, 2016M590422), the Natural Science
458 Foundation of Jiangsu Province (BK20160506, BE2016306), International Science and
459 Technology Cooperation Project of Jiangsu Province (BZ2016013), Suzhou Science and
460 Technology Project (SNG201503) and Priority Academic Program Development of
461 Jiangsu Higher Education Institutions (PAPD). We also would like to thank our colleagues
462 in School of Food and Biological Engineering who provided assistance in this study.

463 **NOTES**

464 The authors declare no competing financial interest.

465 **Supporting Information description**

466 There were two figures in the supporting information file. Fig. S1 the photo of the
467 device that was used to detect milk and fish spoilage. Fig. S2 was the change of the R,
468 G, and B values of written patterns “F” on the GGG-RRA10 film used to monitor milk
469 and fish spoilage.

470

471 **REFERENCES**

- 472 1. Realini, C. E.; Marcos, B., Active and intelligent packaging systems for a modern society.
473 *Meat Sci.* **2014**, *98*, 404-19.
- 474 2. Ghaani, M.; Cozzolino, C. A.; Castelli, G.; Farris, S., An overview of the intelligent
475 packaging technologies in the food sector. *Trends Food Sci. Technol.* **2016**, *51*, 1-11.
- 476 3. Pacquit, A.; Frisby, J.; Diamond, D.; Lau, K.; Farrell, A.; Quilty, B.; Diamond, D.,
477 Development of a smart packaging for the monitoring of fish spoilage. *Food Chem.* **2007**, *102*,
478 466-470.
- 479 4. Rukchon, C.; Nopwinyuwong, A.; Trevanich, S.; Jinkarn, T.; Suppakul, P., Development of
480 a food spoilage indicator for monitoring freshness of skinless chicken breast. *Talanta* **2014**, *130*,
481 547-54.
- 482 5. Dainelli, D.; Gontard, N.; Spyropoulos, D.; Zondervan-van den Beuken, E.; Tobback, P.,
483 Active and intelligent food packaging: legal aspects and safety concerns. *Trends Food Sci.*
484 *Technol.* **2008**, *19*, S103-S112.
- 485 6. Zhang, X.; Lu, S.; Chen, X., A visual pH sensing film using natural dyes from *Bauhinia*
486 *blakeana* Dunn. *Sensors Actuators B: Chem.* **2014**, *198*, 268-273.
- 487 7. Luchese, C. L.; Abdalla, V. F.; Spada, J. C.; Tessaro, I. C., Evaluation of blueberry residue
488 incorporated cassava starch film as pH indicator in different simulants and foodstuffs. *Food*
489 *Hydrocoll.* **2018**, *82*, 209-218.
- 490 8. Pereira, V. A.; de Arruda, I. N. Q.; Stefani, R., Active chitosan/PVA films with
491 anthocyanins from *Brassica oleraceae* (Red Cabbage) as Time–Temperature Indicators for
492 application in intelligent food packaging. *Food Hydrocoll.* **2015**, *43*, 180-188.
- 493 9. Saliu, F.; Della Pergola, R., Carbon dioxide colorimetric indicators for food packaging
494 application: Applicability of anthocyanin and poly-lysine mixtures. *Sensors Actuators B: Chem.*
495 **2018**, *258*, 1117-1124.
- 496 10. Silva-Pereira, M. C.; Teixeira, J. A.; Pereira-Júnior, V. A.; Stefani, R., Chitosan/corn starch
497 blend films with extract from *Brassica oleraceae* (red cabbage) as a visual indicator of fish
498 deterioration. *LWT - Food Sci. Technol.* **2015**, *61*, 258-262.
- 499 11. Wei, Y.-C.; Cheng, C.-H.; Ho, Y.-C.; Tsai, M.-L.; Mi, F.-L., Active gellan gum/purple sweet
500 potato composite films capable of monitoring pH variations. *Food Hydrocoll.* **2017**, *69*, 491-502.
- 501 12. Zhai, X.; Shi, J.; Zou, X.; Wang, S.; Jiang, C.; Zhang, J.; Huang, X.; Zhang, W.; Holmes, M.,
502 Novel colorimetric films based on starch/polyvinyl alcohol incorporated with roselle
503 anthocyanins for fish freshness monitoring. *Food Hydrocoll.* **2017**, *69*, 308-317.
- 504 13. Ma, Q.; Wang, L., Preparation of a visual pH-sensing film based on tara gum
505 incorporating cellulose and extracts from grape skins. *Sensors Actuators B: Chem.* **2016**, *235*,
506 401-407.
- 507 14. Ma, Q.; Ren, Y.; Gu, Z.; Wang, L., Developing an intelligent film containing *Vitis*
508 *amurensis* husk extracts: The effects of pH value of the film-forming solution. *J. Clean. Prod.*
509 **2017**, *166*, 851-859.
- 510 15. Kuswandi, B.; Jayus; Larasati, T. S.; Abdullah, A.; Heng, L. Y., Real-Time Monitoring of
511 Shrimp Spoilage Using On-Package Sticker Sensor Based on Natural Dye of Curcumin. *Food Anal.*
512 *Methods* **2011**, *5*, 881-889.
- 513 16. Ma, Q.; Du, L.; Wang, L., Tara gum/polyvinyl alcohol-based colorimetric NH₃ indicator
514 films incorporating curcumin for intelligent packaging. *Sensors Actuators B: Chem.* **2017**, *244*,
515 759-766.

- 516 17. Liu, J.; Wang, H.; Wang, P.; Guo, M.; Jiang, S.; Li, X.; Jiang, S., Films based on κ -
517 carrageenan incorporated with curcumin for freshness monitoring. *Food Hydrocoll.* **2018**.
- 518 18. Musso, Y. S.; Salgado, P. R.; Mauri, A. N., Smart edible films based on gelatin and
519 curcumin. *Food Hydrocoll.* **2017**, *66*, 8-15.
- 520 19. Otsuki, T.; Matsufuji, H.; Takeda, M.; Toyoda, M.; Goda, Y., Acylated anthocyanins from
521 red radish (*Raphanus sativus* L.). *Phytochemistry* **2002**, *60*, 79-87.
- 522 20. Matsufuji, H.; Kido, H.; Misawa, H.; Yaguchi, J.; Otsuki, T.; Chino, M.; Takeda, M.;
523 Yamagata, K., Stability to Light, Heat, and Hydrogen Peroxide at Different pH Values and DPPH
524 Radical Scavenging Activity of Acylated Anthocyanins from Red Radish Extract. *J. Agric. Food.*
525 *Chem.* **2007**, *55*, 3692-3701.
- 526 21. Park, N. I.; Xu, H.; Li, X.; Jang, I. H.; Park, S.; Ahn, G. H.; Lim, Y. P.; Kim, S. J.; Park, S. U.,
527 Anthocyanin Accumulation and Expression of Anthocyanin Biosynthetic Genes in Radish
528 (*Raphanus sativus*). *J. Agric. Food. Chem.* **2011**, *59*, 6034-6039.
- 529 22. Martucci, J. F.; Accareddu, A. E. M.; Ruseckaite, R. A., Preparation and characterization
530 of plasticized gelatin films cross-linked with low concentrations of Glutaraldehyde. *J. Mater. Sci.*
531 **2012**, *47*, 3282-3292.
- 532 23. Guo, J.; Ge, L.; Li, X.; Mu, C.; Li, D., Periodate oxidation of xanthan gum and its
533 crosslinking effects on gelatin-based edible films. *Food Hydrocoll.* **2014**, *39*, 243-250.
- 534 24. Boateng, J.; Burgos-Amador, R.; Okeke, O.; Pawar, H., Composite alginate and gelatin
535 based bio-polymeric wafers containing silver sulfadiazine for wound healing. *Int. J. Biol.*
536 *Macromol.* **2015**, *79*, 63-71.
- 537 25. Samp, M. A.; Iovanac, N. C.; Nolte, A. J., Sodium Alginate Toughening of Gelatin
538 Hydrogels. *ACS Biomater. Sci. Eng.* **2017**, *3*.
- 539 26. Qiao, C.; Ma, X.; Zhang, J.; Yao, J., Molecular interactions in gelatin/chitosan composite
540 films. *Food Chem.* **2017**, *235*, 45-50.
- 541 27. Zia, K. M.; Tabasum, S.; Khan, M. F.; Akram, N.; Akhter, N.; Noreen, A.; Zuber, M., Recent
542 trends on gellan gum blends with natural and synthetic polymers: A review. *Int. J. Biol.*
543 *Macromol.* **2018**, *109*, 1068-1087.
- 544 28. Ferris, C. J.; Gilmore, K. J.; Wallace, G. G.; Panhuis, M. I. H., Modified gellan gum
545 hydrogels for tissue engineering applications. *Soft Matter* **2013**, *9*, 3705-3711.
- 546 29. Lee, K. Y.; Shim, J.; Lee, H. G., Mechanical properties of gellan and gelatin composite
547 films. *Carbohydr. Polym.* **2004**, *56*, 251-254.
- 548 30. Xu, X.-J.; Fang, S.; Li, Y.-H.; Zhang, F.; Shao, Z.-P.; Zeng, Y.-T.; Chen, J.; Meng, Y.-C., Effects
549 of low acyl and high acyl gellan gum on the thermal stability of purple sweet potato
550 anthocyanins in the presence of ascorbic acid. *Food Hydrocoll.* **2018**.
- 551 31. Robert, T., "Green ink in all colors"—Printing ink from renewable resources. *Prog. Org.*
552 *Coat.* **2015**, *78*, 287-292.
- 553 32. Aznar, M.; Domeño, C.; Nerín, C.; Bosetti, O., Set-off of non volatile compounds from
554 printing inks in food packaging materials and the role of lacquers to avoid migration. *Dyes and*
555 *Pigments* **2015**, *114*, 85-92.
- 556 33. Wang, H.; Qian, J.; Li, H.; Ding, F., Rheological characterization and simulation of
557 chitosan-TiO₂ edible ink for screen-printing. *Prog. Org. Coat.* **2018**, *120*, 19-27.
- 558 34. Wu, S.; Wang, W.; Yan, K.; Ding, F.; Shi, X.; Deng, H.; Du, Y., Electrochemical writing on
559 edible polysaccharide films for intelligent food packaging. *Carbohydr. Polym.* **2018**, *186*, 236-
560 242.
- 561 35. Wang, Z.; Li, Y.; Chen, L.; Xin, X.; Yuan, Q., A study of controlled uptake and release of
562 anthocyanins by oxidized starch microgels. *J. Agric. Food. Chem.* **2013**, *61*, 5880-7.

- 563 36. Xiaowei, H.; Xiaobo, Z.; Jiewen, Z.; Jiyong, S.; Zhihua, L.; Tingting, S., Monitoring the
564 biogenic amines in Chinese traditional salted pork in jelly (Yao-meat) by colorimetric sensor
565 array based on nine natural pigments. *Int. J. Food Sci. Tech.* **2015**, *50*, 203-209.
- 566 37. Lixin, L.; Weizhou, Z.; Zhiye, L.; Yali, T., Development and Application of Time–
567 temperature Indicators Used on Food during the Cold Chain Logistics. *Packag. Technol. Sci.*
568 **2013**, *26*, 80-90.
- 569 38. Cai, J.; Chen, Q.; Wan, X.; Zhao, J., Determination of total volatile basic nitrogen (TVB-N)
570 content and Warner-Bratzler shear force (WBSF) in pork using Fourier transform near infrared
571 (FT-NIR) spectroscopy. *Food Chem.* **2011**, *126*, 1354-1360.
- 572 39. Choi, I.; Lee, J. Y.; Lacroix, M.; Han, J., Intelligent pH indicator film composed of
573 agar/potato starch and anthocyanin extracts from purple sweet potato. *Food Chem.* **2017**, *218*,
574 122-128.
- 575 40. Pranoto, Y.; Lee, C. M.; Park, H. J., Characterizations of fish gelatin films added with
576 gellan and κ -carrageenan. *LWT - Food Sci. Technol.* **2007**, *40*, 766-774.
- 577 41. Fonkwe, L. G.; Narsimhan, G.; Cha, A. S., Characterization of gelation time and texture of
578 gelatin and gelatin–polysaccharide mixed gels. *Food Hydrocoll.* **2003**, *17*, 871-883.
- 579 42. Jin, W.; Shih - Chien, C.; M., P. E.; K., K. T., Effects of phenolic compounds on gelation
580 behavior of gelatin gels. *J. Polym. Sci., Part A: Polym. Chem.* **2001**, *39*, 224-231.
- 581 43. Picone, C. S. F.; Cunha, R. L., Influence of pH on formation and properties of gellan gels.
582 *Carbohydr. Polym.* **2011**, *84*, 662-668.
- 583 44. Jiang, Y.; Li, Y.; Zhi, C.; Leng, X., Study of the Physical Properties of Whey Protein Isolate
584 and Gelatin Composite Films. *J. Agric. Food. Chem.* **2010**, *58*, 5100-5108.
- 585 45. Bitencourt, C. M.; Fávoro-Trindade, C. S.; Sobral, P. J. A.; Carvalho, R. A., Gelatin-based
586 films additivated with curcuma ethanol extract: Antioxidant activity and physical properties of
587 films. *Food Hydrocoll.* **2014**, *40*, 145-152.
- 588 46. Prodpran, T.; Benjakul, S.; Phatcharat, S., Effect of phenolic compounds on protein
589 cross-linking and properties of film from fish myofibrillar protein. *Int. J. Biol. Macromol.* **2012**,
590 *51*, 774-782.
- 591 47. Parris, N.; Coffin, D. R.; RF, J.; H, P., Composition factors affecting the water vapor
592 permeability and tensile properties of hydrophilic films. *J. Agric. Food Chem.* **1997**, *45*, 1596-
593 1599.
- 594 48. Jakobek, L., Interactions of polyphenols with carbohydrates, lipids and proteins. *Food*
595 *Chem.* **2015**, *175*, 556-567.
- 596 49. Garusinghe, U. M.; Varanasi, S.; Raghuvanshi, V. S.; Garnier, G.; Batchelor, W.,
597 Nanocellulose-montmorillonite composites of low water vapour permeability. *Colloids Surf.*
598 *Physicochem. Eng. Aspects* **2018**, *540*, 233-241.
- 599 50. Castañeda-Ovando, A.; Pacheco-Hernández, M. d. L.; Páez-Hernández, M. E.; Rodríguez,
600 J. A.; Galán-Vidal, C. A., Chemical studies of anthocyanins: A review. *Food Chem.* **2009**, *113*, 859-
601 871.
- 602 51. Torskangerpoll, K.; Andersen, O. M., Colour stability of anthocyanins in aqueous
603 solutions at various pH values. *Food Chem.* **2005**, *89*, 427-440.
- 604

605 **Figure captions**

606 **Fig. 1.** The color (A) and UV-vis spectra (B) of RRA anthocyanins extract solution at pH 2-12, and
607 the color (C) and UV-vis spectra (D) of GGG-RRA10 film at pH 2-12. Insets of (B) and (D) were
608 the change of A_{580}/A_{510} of the RRA solution and GGG-RRA10 film with the change of pH,
609 respectively.

610 **Fig. 2.** The SEM images of cross sections of GGG (A), GGG-RRA5 (B), GGG-RRA10 (C), GGG-
611 RRA15 (D) and GGG-RRA20 film (E).

612 **Fig. 3.** The mechanical properties (A), transparencies (B), WVP (C) and OP (D) of the GGG and
613 GGG-RRA films.

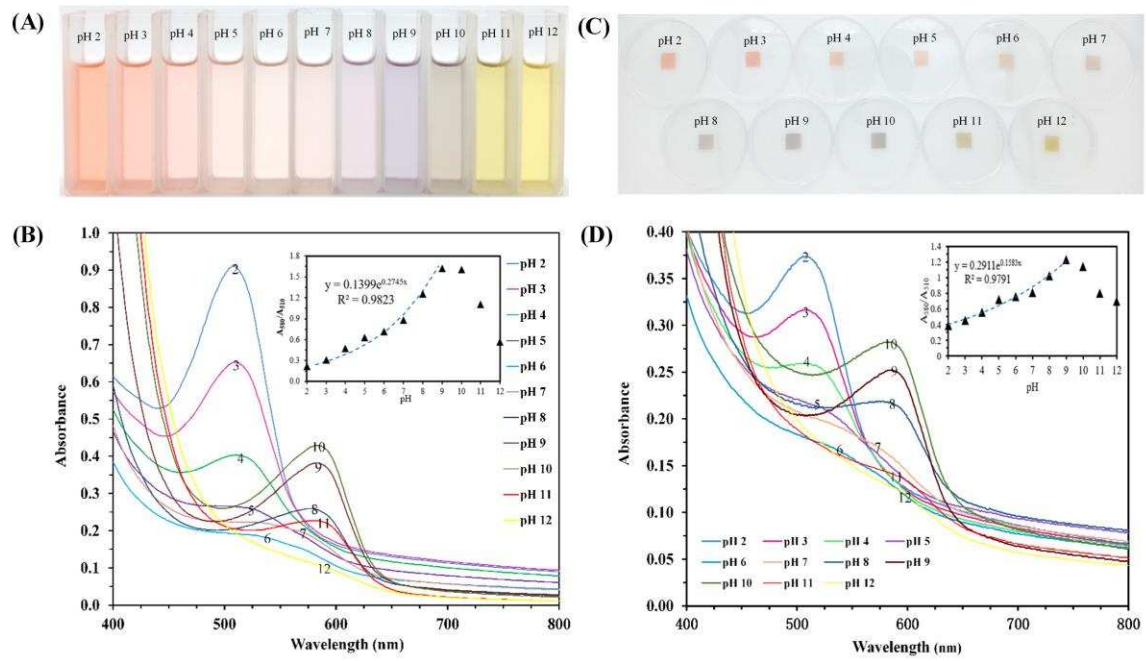
614 **Scheme 1.** The principle of electrochemical writing on GGG-RRA film.

615 **Fig. 4.** The photo of GGG-RRA10 hydrogel (A); the images of pattern “1” at different current
616 magnitude when the Pt needle was connected with the anode (B) and cathode (C) of the
617 electrochemical workstation; the images of multicolor pattern flower (D) and apple (E) written on
618 the film.

619 **Fig. 5.** Images (A) and the corresponding S values (B) of the GGG-RRA10 film with written patterns
620 stored at 4, 25 and 37 °C for 30 days; the color response of the GGG-RRA10 film with written
621 patterns towards acetic acid (C) and ammonia gas (D).

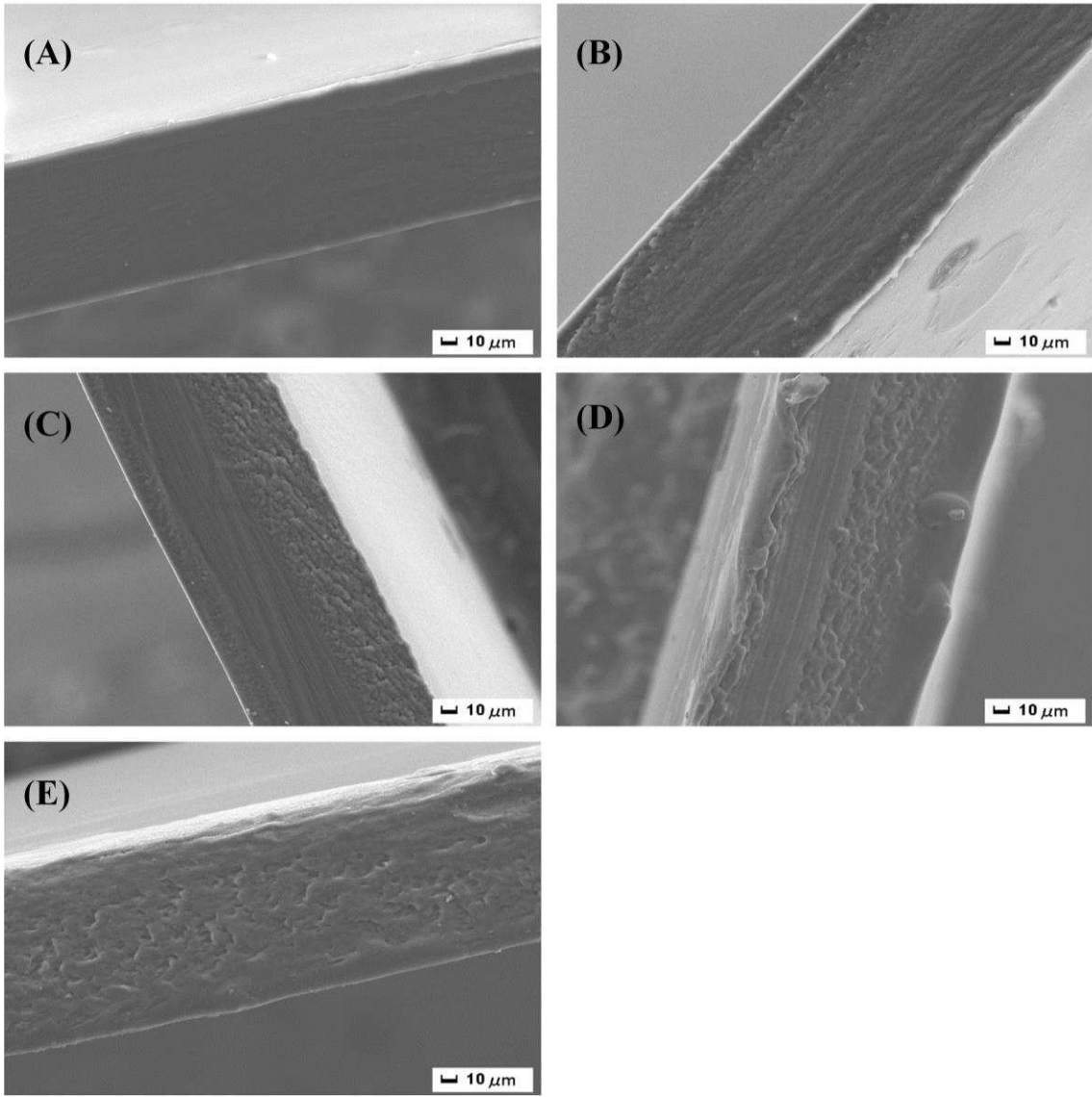
622 **Fig. 6.** Images of GGG-RRA10 film with red pattern “F” when used to monitor the milk spoilage
623 at 25 °C (A), and the corresponding R, G, B values changes of the film and the acidity change of
624 the milk (B); Images of GGG-RRA10 film with yellow pattern “F” when used to monitor the black
625 carp spoilage at 4 °C (C), and the corresponding R, G, B value changes of the film and the TVB-N
626 content changes of the black carp (D).

627 Figure 1.



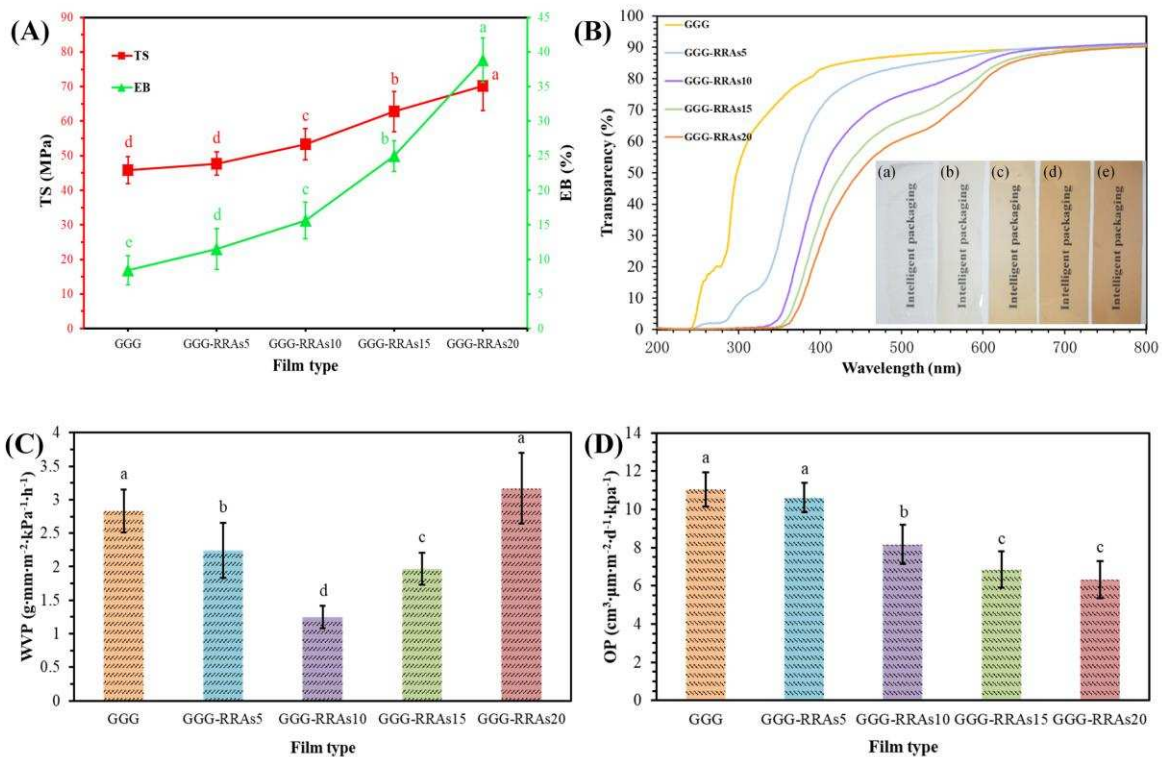
628

629 Figure 2.



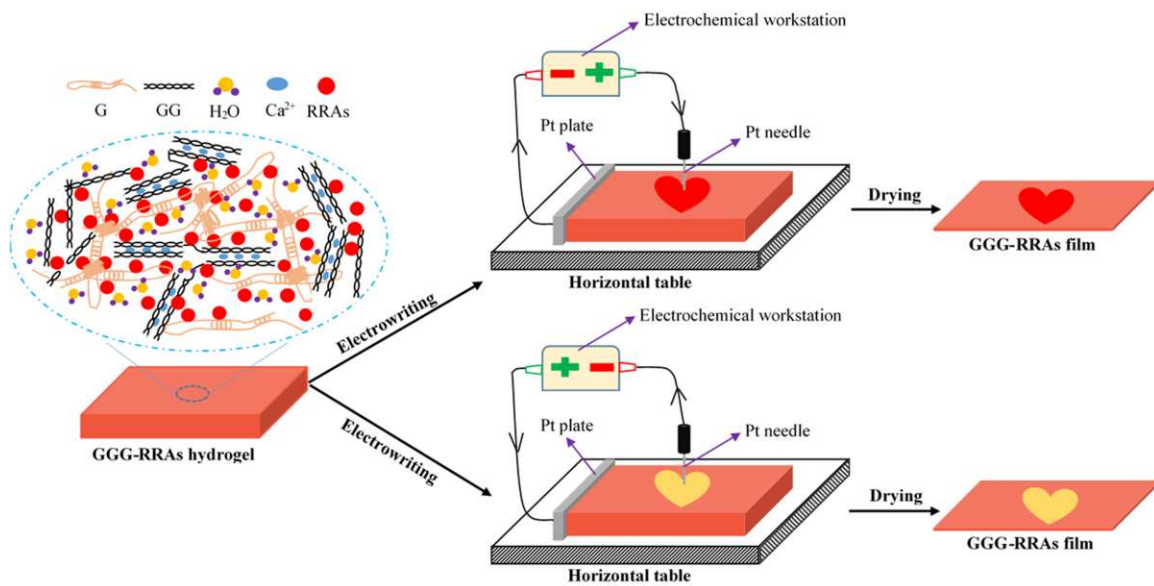
630

631 Figure 3.

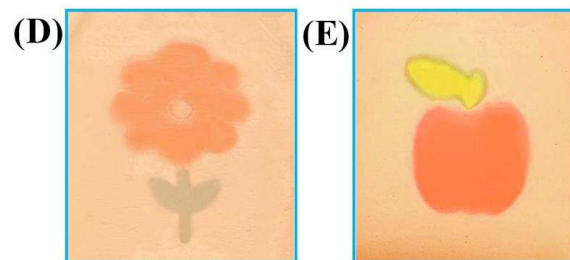
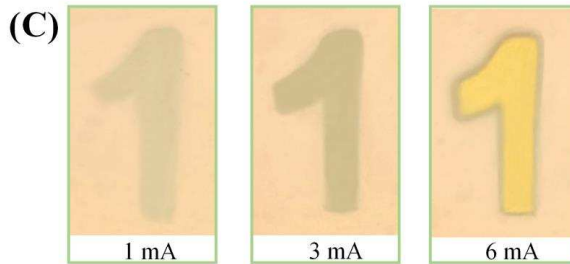
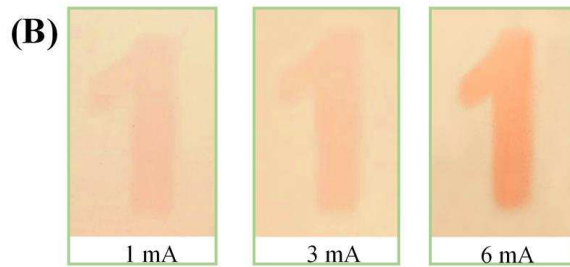
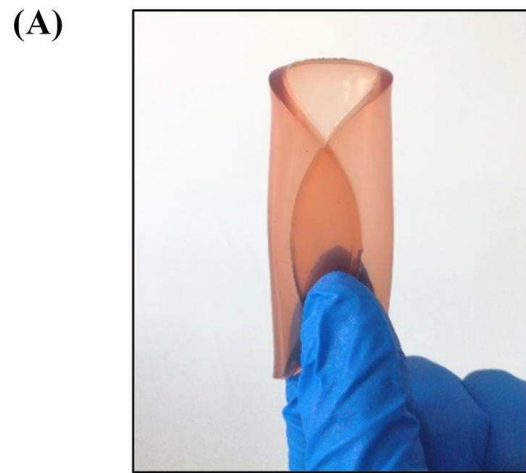


632

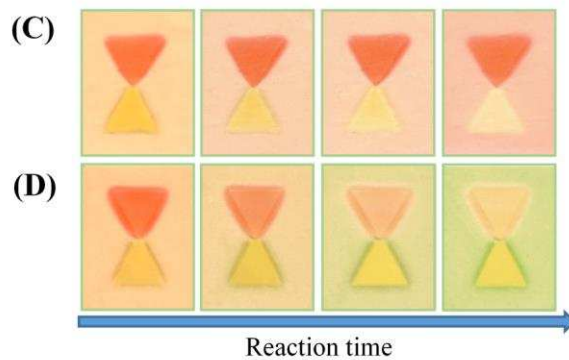
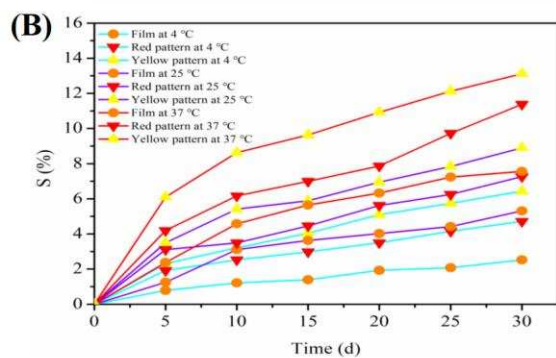
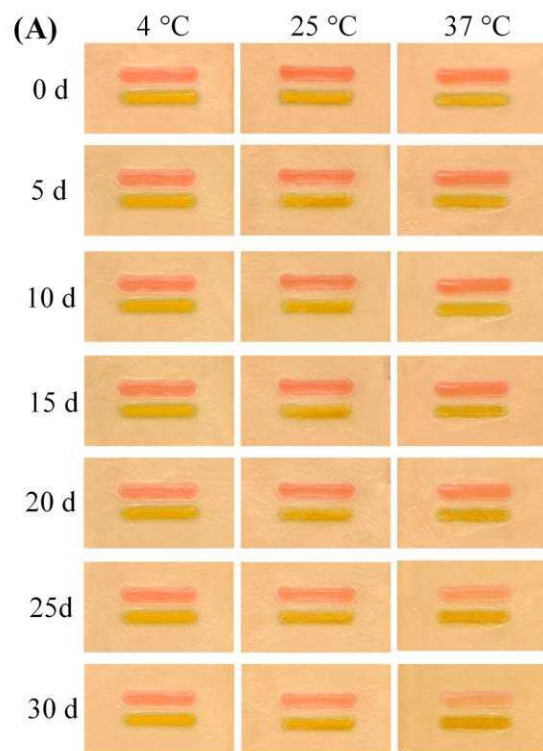
633 Scheme 1.



634

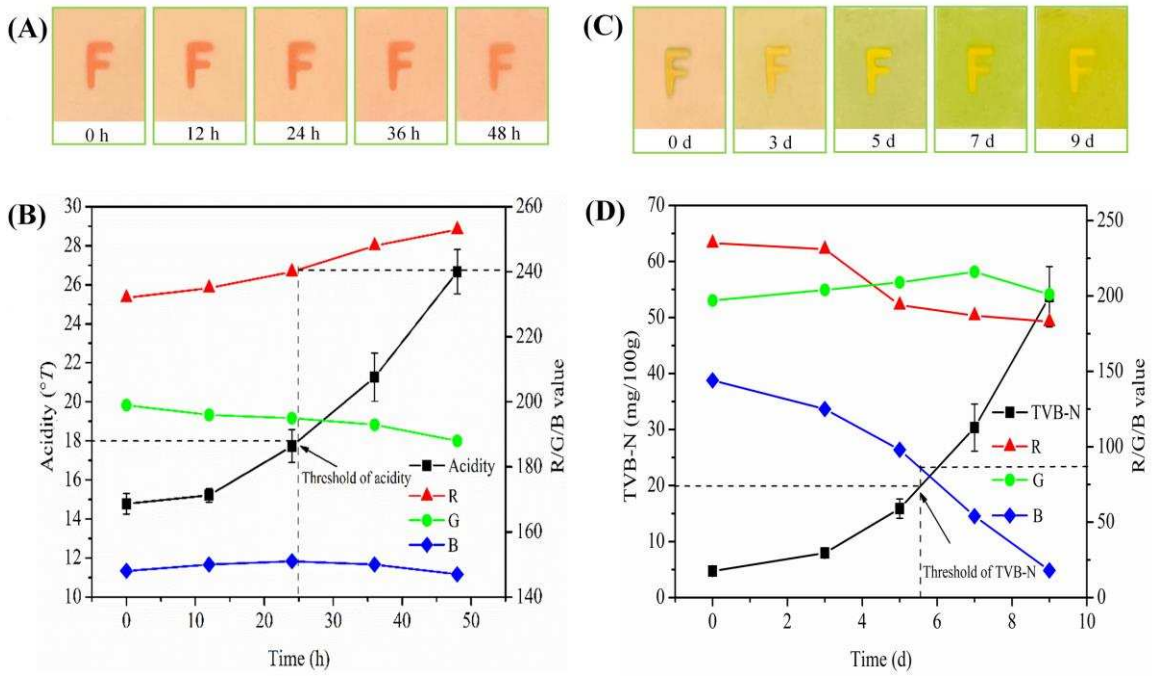


637 Figure 5.



638

639 Figure 6.



640